

Theoretical performance of mid-infrared broken-gap multilayer superlattice lasers

Michael E. Flatté,^{a)} J. T. Olesberg, S. A. Anson, and Thomas F. Boggess
Department of Physics and Astronomy, University of Iowa, Iowa City, Iowa 52242

T. C. Hasenberg and R. H. Miles^{b)}
Hughes Research Laboratories, Malibu, California 90265

C. H. Grein
Physics Department M/C 273, University of Illinois at Chicago, Chicago, Illinois 60607-7059

(Received 10 March 1997; accepted for publication 15 April 1997)

We present calculations of the differential gain and threshold current densities for a 3.7 μm multiple quantum well structure consisting of a “well” composed of several periods of an InAs/InGaSb superlattice alternating with a quaternary alloy “barrier.” We find serious limitations to the optical properties of active regions composed of these multiple quantum wells, and propose a four-layer superlattice structure which corrects these problems. © 1997 American Institute of Physics. [S0003-6951(97)03024-6]

Commercial and military interest in mid-infrared lasers has spawned research efforts focusing on a few promising strategies for constructing a laser active region. These include quantum well^{1,2} and superlattice^{3,4} active regions in which light is created during an interband recombination event, and quantum cascade structures,⁵ in which the radiative transition is intersubband. For the first two categories the expected dominant nonradiative carrier loss mechanism near room temperature is carrier-carrier (Auger) scattering, while in the cascade lasers it is electron-phonon scattering.

Design strategies to reduce the Auger recombination rate have been developed for superlattice active regions based on alternating layers of InAs and InGaSb.⁶ These include attempts to (1) lower the density of states at the valence edge and thus decrease the threshold carrier concentration, and (2) to eliminate final states for Auger processes within the conduction and valence bands. Figure 1 shows a typical design: a superlattice of 12.5 Å thick InAs layers alternating with 39 Å thick In_{0.25}Ga_{0.75}Sb layers.⁷ This structure has a relatively light in-plane mass ($m=0.044m_0$, where m_0 is the free mass) for the top valence band. Since the HH3—HH1 matrix elements are very small at the zone center, Auger transitions which excite a hole from HH1 to HH3 are negligible for small in-plane momenta. Hence this superlattice effectively lacks final states at the resonant energies for Auger transitions in the conduction and valence bands.

Unfortunately the above superlattice cannot be grown thick enough for a laser active region, since it is not lattice-matched to a useful substrate. This problem applies to all two-layer superlattices with the above layer compositions and band gaps in the mid-wavelength infrared. The strategy adopted for growing structures approximating the above system is to alternate several periods of the superlattice with a strain-compensating barrier material.³ We will refer to this structure as a superlattice multiple quantum well (MQW).

Previous theoretical work on these structures approximated the thin superlattice layer as a thick layer, or at best as

a thin layer of effective continuous (unstructured) material in a quantum well. We show that the superlattice MQW growth strategy produces several unfavorable effects within the electronic structure of the active region which have been neglected by previous theoretical calculations. These include a large mismatch between the conduction and valence density of states, weak overlap of states at the edges of the valence band and conduction band, and substantial intersubband absorption at the lasing energy. The mismatch in the density of states leads to higher threshold carrier densities, Auger recombination rates, and threshold current densities, while the weak overlap of the band-edge states and the substantial intersubband absorption lead to unacceptably small differential gains. We propose a new four-layer superlattice which circumvents the shortcomings of the superlattice MQW and should in fact outperform thick InAs/InGaSb superlattices. The new structure also balances stresses at a sufficiently microscopic level to suppress the formation of misfit defects.

In Fig. 2(a) we show the band-edge alignment for a representative 3.7 μm superlattice MQW, consisting of 4.5 peri-

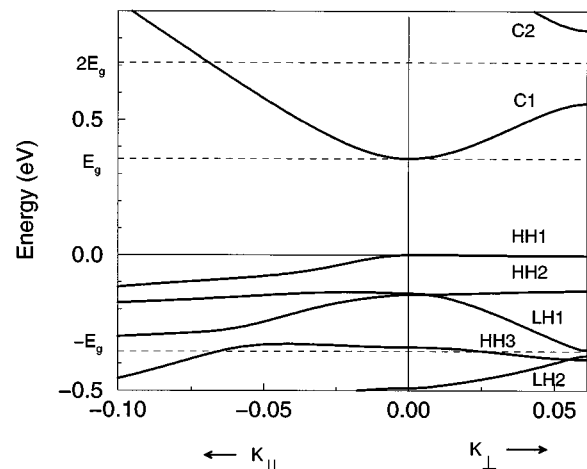


FIG. 1. 300 K band structure of a 12.5 Å InAs/39 Å In_{0.25}Ga_{0.75}Sb superlattice. K_{\perp} is in the growth direction and K_{\parallel} is in the in-plane direction. The resonant energies for processes involving two nonequilibrium holes ($-E_g$) and two nonequilibrium electrons ($2E_g$) are indicated by the dashed lines.

^{a)}Electronic mail: flatte@rashi.physics.uiowa.edu

^{b)}Present address: SDL Inc., 80 Orchard Way, San Jose, CA 95134-1365.

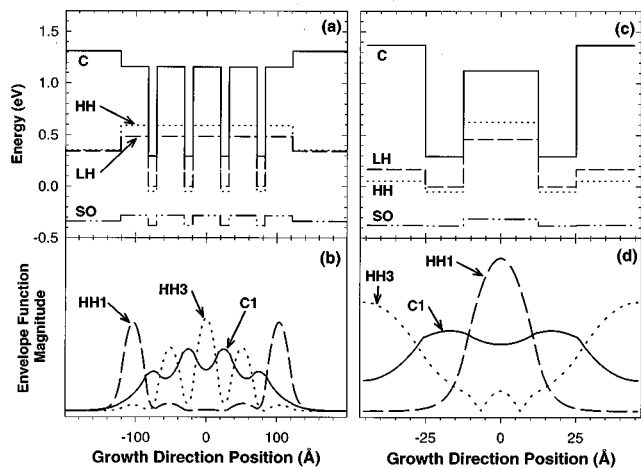


FIG. 2. 300 K band alignment (a) and envelope functions (b) for a 4.5 period 15 \AA InAs/ 36 \AA $\text{In}_{0.25}\text{Ga}_{0.75}\text{Sb}$ superlattice with 400 \AA $\text{Al}_{0.2}\text{Ga}_{0.6}\text{In}_{0.2}\text{As}_{0.17}\text{Sb}_{0.83}$ barriers. Band alignment (c) and envelope functions (d) for a four-layer superlattice consisting of 24 \AA InAs/ 13.8 \AA $\text{In}_{0.4}\text{Ga}_{0.6}\text{Sb}/24 \text{ \AA}$ InAs/ 40 \AA $\text{Al}_{0.3}\text{In}_{0.28}\text{As}_{0.5}\text{Sb}_{0.5}$. Since the C1 state is composed of envelope functions from the bulk conduction, light-hole and split-off bands, the magnitude of the envelope function vector is shown. Zero energy is the light-hole energy in the strained InAs layer.

ods of a 15 \AA InAs/ 36 \AA $\text{In}_{0.25}\text{Ga}_{0.75}\text{Sb}$ superlattice (terminating with InGaSb layers), alternating with 400 \AA barriers of $\text{Al}_{0.2}\text{Ga}_{0.6}\text{In}_{0.2}\text{As}_{0.17}\text{Sb}_{0.83}$.^{8,9} The C1, HH1, and HH3 subband envelope function magnitudes are shown in Fig. 2(b). Calculations of the electronic structure were performed within an envelope-function approximation and using a superlattice $\mathbf{K}\cdot\mathbf{p}$ technique similar to that used in Ref. 10 but generalized to an arbitrary number of layers in the unit cell. Since the “wells” of the superlattice MQW terminate with $\text{In}_{0.25}\text{Ga}_{0.75}\text{Sb}$ layers and the quinary layer does not confine holes as well as the InAs layers, the top two heavy-hole states are localized in the *outer* InGaSb layers. As shown in Fig. 2(b) the HH1 state does not overlap strongly with the C1 state — it is the HH3 state which has the largest overlap.

Several elements of the band structure of the superlattice MQW [shown in Fig. 3(a)] are unfavorable for laser performance. The HH1-HH5 splitting is 6 meV , so the five top heavy-hole subbands (one for each ternary layer) are approximately equally occupied at room temperature. In contrast, only C1 is well-occupied at room temperature and lasing densities. Carriers in the HH1, HH2, and HH4 states will not contribute efficiently to the gain due to their small overlap with C1, but will degrade laser performance through enhancing the possibilities for nonradiative recombination and intersubband absorption. The multiplicity of the band-edge heavy-hole subbands contributes to a large imbalance between the valence density of states and conduction density of states, which enhances the Auger rates.

Another unpleasant feature of the band structure of Fig. 3(a) is that there are no evident gaps near the resonant energies for Auger transitions. Such gaps of the suppression of Auger recombination are eliminated due to the multitude of quantum well subbands.

We propose a new superlattice with a four-layer repeating unit cell consisting of 24 \AA InAs/ 13.8 \AA $\text{In}_{0.4}\text{Ga}_{0.6}\text{Sb}/24 \text{ \AA}$ InAs/ 40 \AA $\text{Al}_{0.3}\text{Ga}_{0.42}\text{In}_{0.28}\text{As}_{0.5}\text{Sb}_{0.5}$ as a superior de-

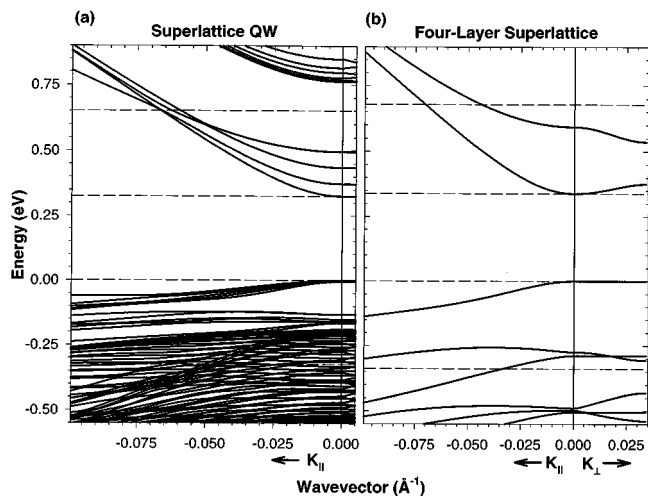


FIG. 3. Comparison of the 300 K band structure of the superlattice MQW of Fig. 2(a) and the four-layer superlattice of Fig. 2(c).

sign for a 3.7 \mu m laser’s active region. Four-layer superlattices where the fourth layer is AlSb have been proposed and grown for optically pumped lasers,⁴ where carrier transport through the active region is not a critical issue. Since our interest is primarily in diodes, our fourth layer has a smaller band gap, allowing conduction states to extend through the entire superlattice unit. However, since the heavy-hole state remains confined in the InGaSb layers, we remain concerned over hole transport through these structures. The quinary layer has tensile strain when grown on GaSb and thus the overall superlattice unit cell (ranging in size from 60 \AA to 110 \AA for band gaps in the $3\text{--}5 \text{ \mu m}$ range) can be lattice matched to GaSb. Strain compensating over this size unit cell may provide better conditions for growth than attempting to compensate strains over $\sim 500 \text{ \AA}$ (as in Ref. 3). Use of the more highly strained $\text{In}_{0.4}\text{Ga}_{0.6}\text{Sb}$ as the ternary layer increases the heavy-hole offset with the other superlattice layers, which clears out final heavy-hole states from around the resonant energy. Further flexibility is available by adjusting the quinary alloy composition.

The band-edge alignment for the four-layer superlattice is shown in Fig. 2(c), and the envelope functions are shown in Fig. 2(d). When strain is taken into account, the heavy-hole band energy difference between the InGaSb layer and the quinary is estimated to be 573 meV , and the conduction band offset between InAs and the quinary is estimated to be 1.045 eV .⁹ The single band-edge heavy-hole state overlaps strongly with C1, yielding a lighter mass and larger matrix elements for band-edge absorption than found for the superlattice MQW.

The band structure for the four-layer superlattice is shown in Fig. 3(b). In contrast to the superlattice MQW, the band-edge valence and conduction subbands of the four-layer superlattice have an in-plane mass ratio of 1.86, where a ratio of 1 is ideal for suppressing Auger processes and achieving large gains. As a result, and also due to the strong C1—HH1 overlap, the band-edge absorption of the four-layer superlattice is five times greater than that of the superlattice MQW. The bandwidth of the C1 state is 37 meV in the growth direction, indicating reasonable transport proper-

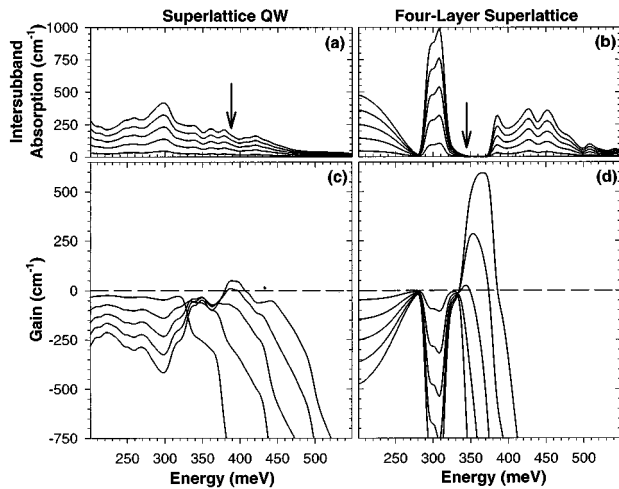


FIG. 4. Intersubband absorption at 300 K for densities of 1, 3, 5, 7, and $9 \times 10^{17} \text{ cm}^{-3}$ for (a) the superlattice MQW and (b) the four-layer superlattice. For an Auger optimized structure, the intersubband absorption (here dominated by intervalence transitions) has a gap at the lasing energy (arrows). Also shown are the gain spectra of the two active regions.

ties at room temperature. The gap in the resonant valence states, 140 meV, is almost an order of magnitude larger than that calculated for the two-layer superlattice (22 meV) shown in Fig. 1. The 50 meV which separates the resonant energy from the nearest band is more than an optical phonon energy, so one might also suppress phonon-assisted Auger processes.

The presence or absence of a gap in the final states within the valence band has a clear effect on the intersubband absorption, shown in Fig. 4 for the superlattice MQW and four-layer superlattice. Intersubband absorption for the superlattice MQW becomes the dominant loss mechanism (140 cm^{-1}) at the threshold carrier density ($7.6 \times 10^{17} \text{ cm}^{-3}$, defined as the density¹¹ required for 25 cm^{-1} gain), and strongly suppresses the gain as is shown in Fig. 4(c). We design the four-layer superlattice with the gain region placed midway between the two intersubband absorption features, as shown in Fig. 4(d), so the intersubband absorption does not suppress the active region's gain. Thus the threshold carrier concentration is lower, $4.7 \times 10^{17} \text{ cm}^{-3}$. By locating the intersubband absorption peaks experimentally one can determine the success of growth and design.

The differential gain for the four-layer superlattice, $1.5 \times 10^{-15} \text{ cm}^{-4}$, is 8 times larger than $1.9 \times 10^{-16} \text{ cm}^{-4}$, that of the superlattice MQW. The difference is due to three effects within the superlattice MQW: the large imbalance in the conduction and valence density of states for the superlattice MQW makes it very difficult to make any part of the valence band degenerate; the small HH1–C1 overlap of the superlattice MQW reduces the magnitude of the gain; and the intersubband absorption is providing an additional loss mechanism for the active region.

The radiative and non-radiative recombination rates, carrier lifetimes, and threshold current densities were calculated with the procedure described in Refs. 6 and 12. The calculated carrier lifetime at threshold is 4.4 ns for the four-layer superlattice, yielding a threshold current density per unit thickness of active region of $1700 \text{ A cm}^2 \mu\text{m}$. The superlat-

tice MQW, due to its multitude of subbands, is computationally intractable at this time.

Recent measurements of the carrier recombination times, carried out with femtosecond pump-probe measurements, indicate that the Auger lifetimes for grown structures corresponding to Fig. 3(a) and Fig. 3(b) are 0.1 and 1.25 ns, respectively, at 300 K and a carrier density of $5 \times 10^{17} \text{ cm}^{-3}$.¹³ The Shockley-Read-Hall lifetimes of the two samples were comparable, 2.8 and 2.5 ns respectively. The calculated Auger lifetime for the four-layer superlattice at this temperature and density is 4.3 ns, which agrees with experiment within the error of these calculations. A laser structure based on the superlattice design of Fig. 3(b) lased at $3.7 \mu\text{m}$ at room temperature when optically pumped¹⁴.

We find that the procedure of growing optimized two-layer superlattices in an MQW structure to compensate strains does not preserve the optimized features of the band structure. We propose a new, four-layer, lattice-matched structure which has calculated properties that are superior to those of the superlattice MQW and even to those of the original two-layer structures. Strain compensating over a shorter unit cell should also improve growth conditions.

This research was supported in part by the National Science Foundation under Grant No. ECS-9406680.

¹H. K. Choi, G. W. Turner, and M. J. Manfra, *Electron. Lett.* **32**, 1296 (1996); H. K. Choi, G. W. Turner, M. J. Manfra, and M. K. Connors, *Appl. Phys. Lett.* **68**, 2936 (1996).

²S. R. Kurtz, R. M. Biefeld, A. A. Allerman, A. J. Howard, M. H. Crawford, and M. W. Pelczynski, *Appl. Phys. Lett.* **68**, 1332 (1996).

³D. H. Chow, R. H. Miles, T. C. Hasenberg, A. R. Kost, Y. H. Zhang, H. L. Dunlap, and L. West, *Appl. Phys. Lett.* **67**, 3700 (1995); T. C. Hasenberg, D. H. Chow, A. R. Kost, R. H. Miles, and L. West, *Electron. Lett.* **31**, 275 (1995).

⁴J. I. Malin, J. R. Meyer, C. L. Felix, J. R. Lindle, L. Goldberg, C. A. Hoffman, and F. J. Bartoli, *Appl. Phys. Lett.* **68**, 2976 (1996); J. R. Meyer, C. A. Hoffman, F. J. Bartoli, and L. R. Ram-Mohan, *Appl. Phys. Lett.* **67**, 757 (1995); J. I. Malin, C. L. Felix, J. R. Meyer, C. A. Hoffman, J. F. Pinto, C.-H. Lin, P. C. Chang, S. J. Murry, and S.-S. Pei, *Electron. Lett.* **32**, 1593 (1996).

⁵J. Faist, F. Capasso, D. L. Sivco, C. Sirtori, A. L. Hutchinson, and A. Y. Cho, *Science* **264**, 553 (1994); J. Faist, F. Capasso, C. Sirtori, D. L. Sivco, A. L. Hutchinson, and A. Y. Cho, *Electron. Lett.* **32**, 560 (1996).

⁶M. E. Flatté, C. H. Grein, H. Ehrenreich, R. H. Miles, and H. Cruz, *J. Appl. Phys.* **78**, 4552 (1995); C. H. Grein, P. M. Young, and H. Ehrenreich, *J. Appl. Phys.* **76**, 1940 (1994).

⁷M. E. Flatté, C. H. Grein, and H. Ehrenreich (unpublished).

⁸Working laser diodes were grown with the less confining $\text{Ga}_{0.75}\text{In}_{0.25}\text{As}_{0.23}\text{Sb}_{0.77}$ as a barrier. Adding aluminum was intended to improve the optical properties of the active region. Although such improvements were evident in differential transmission measurements, the diodes did not lase, probably due to problems with carrier injection.

⁹Parameters for this quinternary were linearly interpolated from those tabulated in Ref. 6, except for the energy gap, which was linearly interpolated from parametrizations of AlInGaAs (Ref. 15) and AlInGaSb (Ref. 16).

¹⁰M. E. Flatté, P. M. Young, L.-H. Peng, and H. Ehrenreich, *Phys. Rev. B* **53**, 1963 (1996).

¹¹We define our densities based on the entire unit cell of the superlattice [102 \AA for Fig. 3(b)] or superlattice quantum well [640 \AA for Fig. 3(a)].

¹²C. H. Grein, P. M. Young, M. E. Flatté, and H. Ehrenreich, *J. Appl. Phys.* **78**, 7143 (1995).

¹³S. A. Anson, J. T. Olesberg, T. F. Boggess, T. C. Hasenberg, M. E. Flatté, and C. H. Grein (unpublished).

¹⁴In addition to the $3.7 \mu\text{m}$ device, a $5.2 \mu\text{m}$ laser operated at 185 K. T. C. Hasenberg, J. T. Olesberg, M. E. Flatté, A. R. Kost, C. Yan, and D. L. McDaniel, Jr. (unpublished).

¹⁵D. Olego, T. Y. Chang, E. Silberg, E. A. Caridi, and A. Pinczuk, *Appl. Phys. Lett.* **41**, 476 (1982).

¹⁶K. Zbitnew and J. C. Woolley, *J. Appl. Phys.* **52**, 6611 (1981).